3D Semi Landmarks-Based Statistical Face Reconstruction

Maxime Berar[1], Michel Desvignes[1], Gérard Bailly[2] and Yohan Payan[3]

[1] Laboratoire des Images et des Signaux, Saint Martin d'Hères, France
[2] Institut de la Communication Parlée, Grenoble, France
[3] Laboratoire TIMC/IMAG, Faculté de Médecine, La Tronche France

The aim of craniofacial reconstruction is to estimate the shape of a face from the shape of the skull. Few works in computerized assisted facial reconstruction have been provided in the past, probably due to technical (poor machine performances and data availability) and theoretical (complexity) reasons. Therefore, the main published works consist in manual reconstructions. In this paper, an original approach proposes first to build a 3D statistical model of the set skull/face from 3D CT scans. Then, a reconstruction method is introduced in order to estimate, from this statistical model, the 3D facial shape of one subject from known skull data.

Keywords: facial reconstruction, statistical model, elastic registration, missing data reconstruction

1. Introduction

Craniofacial reconstruction can be considered, when confronted with an unrecognizable corpse and when no other identification evidence is available. In such cases the skeletal remains are all that is available to try to create a picture of that person. The aim of craniofacial reconstruction is then to produce a likeness of the face using the skeletalized remains. This reconstruction may hopefully provide a route to a positive identification.

Several 3D manual methods for facial reconstruction have been developed and are currently used in practice. They consist of modeling a face on the remaining skull by use of clay and plasticine. However, manual reconstruction methods have several fundamental shortcomings, such as being highly subjective, time-consuming and requiring artistic talent. Computer-based methods were developed trying to complement or even provide an answer to these shortcomings.

Some current computerized techniques either fit a template skin surface to a set of interactively placed virtual dowels on a 3D digitized model of the remaining skull [1] – [5]. Other ones propose to deform a reference skull in order to match the remaining skull, thanks to crest lines (lines of maximal local curvature) [6], control data sets [7] or feature points [8]. Then they apply an extrapolation of the calculated skull deformation to the template skin surface associated to the reference skull. For both techniques, the template skin or reference skull can either be a generic surface or a specific best look-alike according to the skull. However, the facial reconstruction is biased by the choice of the reference skull and the template skin. Moreover, the model of deformations between skull landmarks and between the reference skull and the template skin is usually quite simple. Recent works using multiple reference skull [9], or a combined statistical deformable model of facial surfaces and tissue thickness [10] addressed the facial reconstruction problem and discussed these bias.

In this paper, a method to build a 3D statistical model of the skull and face is presented. This model is then used to reconstruct a face from available skull data. The idea is similar to [6-8] but uses a statistical shape model of the skull and the face for the reconstruction task, instead of an extrapolation of the deformation field. A 3D-to-3D matching procedure delivers meshes of the skull and face with the same number of vertices via template skull and face. The deformation of the template skull is then used to register the "remaining" skull in our model referential, delivering a "remaining" skull mesh with the same number of vertices as the template mesh. Indeed, all the matched vertices should refer to identical – in structural terms - facial and bony landmarks. Applied to several individuals, a statistical model of the variability of the skull and the face is therefore build. The reconstruction of the face is then resolved using the direct statistical relationship between skin and skull surface shapes given by the statistical model and can be seeing as a missing data problem.

This paper describes our approach for facial reconstruction. Section 2 describes the elaboration of the normalized skull and face geometries, obtained using a 3D-to-3D matching procedure. Section 3 presents the statistical model built upon the normalized

faces and skulls. Finally, section 4 introduces the facial reconstruction method and presents results and sketches some guideline for further improvements.

2. Skull and Face Database

An entry (i.e. a sample) in our database consists of a skull surface coupled with a skin surface. For facial reconstruction, only the skull surface is known. This surface is represented by a 3D mesh (vertices and triangles). In order to construct the statistical model, each skull or skin shape should share the same mesh structure with the same number of vertices. Then, each mesh needs to be registrated in a subject-shared reference system (Figure 1, 3D subject-specific mesh i).

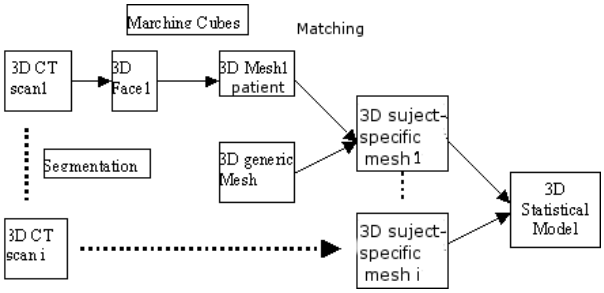

Figure 1. Building a 3D statistical model from 3D CT Scans. A 3D-to-3D matching procedure delivers meshes with the same number of vertices. The matched vertices should refer to identical – in structural terms - facial and bony landmarks..

In this method, the triangles for a region of the skull or the face are supposed to be the same for all samples, while the variability of the position of the vertices will reflect the anatomical characteristics of each sample. The vertex of these shared meshes can be considered as semi-landmarks, i.e. as points that do not have names but that correspond across all the samples of a data set under a reasonable model of deformation from their common mean [11]. The shared meshes are obtained by matching reference meshes of the skull and the skin (see Figure 1 and Figure 2) to several individual meshes using a 3D-to-3D matching algorithm.

2.1. Acquisition and Segmentation

Coronal CT slices (see Figure 2.a) were collected for the partial skulls and faces of 15 subjects (helical scan with a 1-mm pitch and slices reconstructed every 0.31 mm or 0.48 mm). The Marching Cubes algorithm [12] has been implemented to reconstruct the skulls and the faces from CT slices on isosurfaces (see Figure 2.b). Subject-specific meshes for the skull, jaw and face have around 180000, 30000 and 22000 vertices. The respective generic meshes from the Visible Woman Project [13] (for the skull and mandible) and from [14] (for the face) have 3473, 1100 (see Figure2.c) and 5828 vertices. The 3D-to-3D matching algorithm described below is used to obtain normalized meshes of these organs.

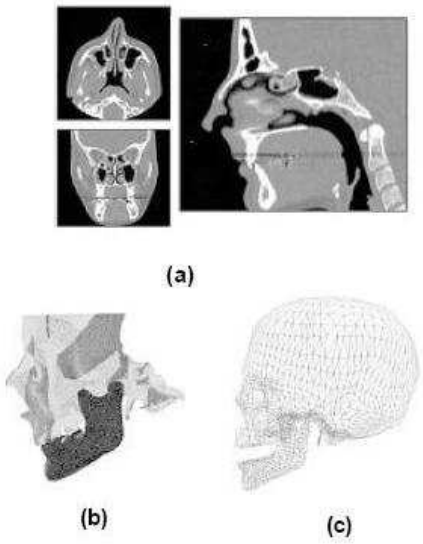

Figure 2. (a) 3D raw scan data (only coronal slices were collected; midsagital and axial have been reconstructed here by image processing), (b) shape reconstructed using the marching cube algorithm [12]; (c) generic mesh obtained from the Visible Woman Project® [13].

Segmentation

Bones and skin volumes are first separated using intensity threshold and morphological operators. Faces volumes are then filled up, with metal artefacts removed manually. The mandible and the skull are separated during the segmentation process because the subjects have different mandible apertures. Skull and mandible are separated semi-automatically using seed growing regions. At the end of the segmentation process, three binary volumes are obtained. The patient meshes are reconstructed for each volume (face, skull, mandible) using a standard Marching Cube algorithm.

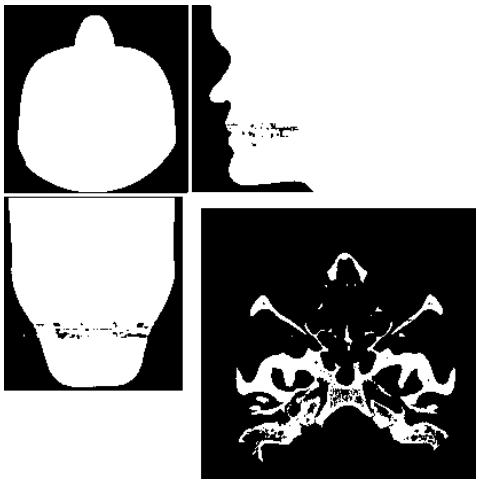

Figure 3. Segmented slides (skin and bone volumes).

Subject-specific meshes

A "symmetric matching" is used to obtain the subject-specific mandible meshes (see section 2.2). Maximal matching errors between the subject-specific meshes and the patient meshes reconstructed from the scans are located on the teeth and on the coronoid process. The mean distances can be considered as the registration noise, due partly to the difference of density (see Table 1.). Teeth will not be part of our model, due to the frequent metal artefacts in CT scans.

Another procedure is used to obtain the subject-specific skulls meshes. Since these data were collected during regular medical exams and excitation of the brain volume is avoided if not necessary, nearly all the skull are partially scanned, and only 2 complete skull and face volume data were available (see an example in Figure 4). Therefore a partial mesh of each skull is first registered on the corresponding part of the 3D generic mesh. "Symmetric matching" (see Section 2.2) insures better registration, as the partial mesh and the original data have equivalent shapes. The rest of the subject skull mesh is obtained by transforming the whole reference skull mesh by this matching process. During this step, the cranial vault is (most of the time) inferred from the border of the skull, using the continuity of the transformation. As this is not so accurate, only the minimal fitting volumes will be used to build the statistical model. The maximal matching errors in the resulting subject-specific skull meshes are located in the spikes beneath the skull, where the individual variability and the surface noise are large, due to segmentation errors.

Finally, face meshes are obtained using the same procedure. In this case, the maximal matching errors between subject-specific and patient meshes are located around the eyes, that are part of the original data, but not part of the generic mesh (see Figure 5 for a distance map between a subject-specific mesh and a patient mesh).). Figure 7 shows 6 of the 15 faces of the database. The template similarity is most seen in the inferred parts of the subject-specific meshes (cranial vaults and necks). Again, only the minimal fitting volumes will be used to build the statistical model.

Table 1. Distance between the patient (subject CT data reconstructed through Marching Cub) and the subject-specific (obtained through registration of the reference meshes) meshes.

Distances (mm)	mean	Max
Mandible	2	8
Skull	4	36
Face	1	5

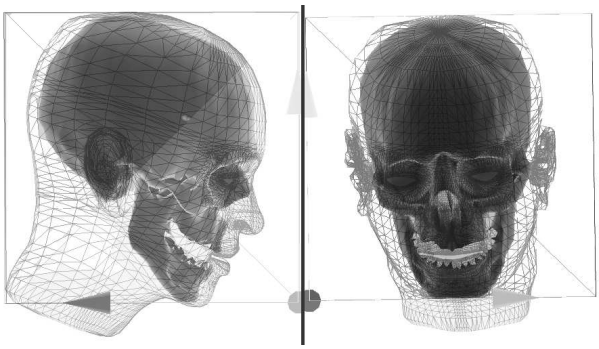

Figure 4. Jaw, skull and face meshes in scan volume.

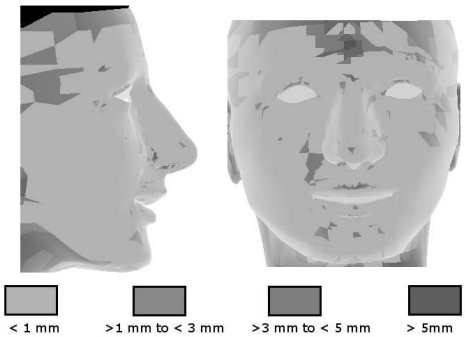

Figure 5. Distance map of a subject-specific face mesh to a patient mesh.

2.2. 3D-to-3D matching

The basic principle of the 3D-to-3D matching procedure [14] consists of the deformation of the initial 3D space by a series of trilinear transformations T_l applied to all vertices q_i of elementary cubes (see Figure 6) of the generic mesh (source) towards the patient mesh (target):

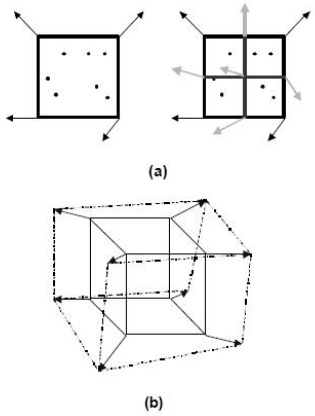

Figure 6. Applying a trilinear transformation to a cube. (a) 2D simplification of a subdivision into 4 elementary volumes of the original space and new transformations vectors; (b) elementary 3D transformation within a cube.

$$T_l(q_i,p)=\begin{bmatrix} p_{00} & p_{01} & & p_{07} \\ p_{10} & p_{11} & \cdots & p_{17} \\ p_{20} & p_{21} & & p_{27} \end{bmatrix}.[1\ x_i\ y_i\ z_i\ x_iy_i\ y_iz_i\ z_ix_i\ x_iy_iz_i]^T$$

The parameters p of each trilinear transformation T_l are computed iteratively using the minimization of a cost function (see Eq.1 below). The elementary cubes are determined by iteratively subdividing the input space (see Figure 3) in order to minimize the distance between the 3D surfaces given by :

(Eq. 1)

$$\min_p \left[\sum_{i=1;i\notin Paired(S_S,S_T)}^{card(S_S)} [d(T(t_i,p),S_S)]^2 + Rw. \sum_{k\in Paired(S_S,S_T)} [d(T(t_k,p),s_k)]^2 + P(p) \right]$$

where S_S is the source surface to be adjusted to the set of points $\{t_i\}$ of the target surface S_T, p are the parameters of the transformations T (6 parameters of the initial rototranslation of the reference coordinate system and 3x8 parameters for each embedded trilinear transformation) applied to the set of points $\{s_i\}$ of S_S. $P(p)$ is a regularization function that guaranties the continuity of the transformations at the limits of each subdivision of the 3D space. It allows larger deformations for smaller subdivisions.

In Eq.1, the first term deals with the distance between the points of the source mesh and the surface of the target mesh, considering the projection of each point onto the deformed surface.

The second term weighted by R_w deals with point-to-point distance: a set of 3D feature points $\{t_k\}$ of the target surface S_T are identified and paired with $\{s_k\}$ vertices of the source surface S_S. R_w decreases with the number of iterations when the source and the target becomes close.

The minimization is performed using the Levenberg-Marquardt algorithm [13].

The problem of matching symmetry [14,15] is encountered, due to the difference of density between the source and target meshes (number of vertices respectively 30 and 70 times larger in the source meshes than in the target meshes). Therefore, the minimization function is symmetrized by adding a term that computes also the distance of the target mesh to the transformed source mesh with the pseudo-inverse transform T^{-1} in the following way:

$$\min_p \left[\begin{array}{l} \sum_{i=1;i\notin Paired(S_T)}^{card(S_T)} \left[d\left(T(t_i,p),S_S\right) \right]^2 + Rw. \sum_{k\in Paired(S_S,S_T)} \left[d\left(T(t_k,p),s_k\right) \right]^2 + P(p) \\ + \sum_{j=1;j\notin Paired(S_S)}^{card(S_S)} \left[d\left(T^{-1}(t_j,p),S_T\right) \right]^2 \end{array} \right]$$

This new distance function solves this matching problem on real skull and face meshes.

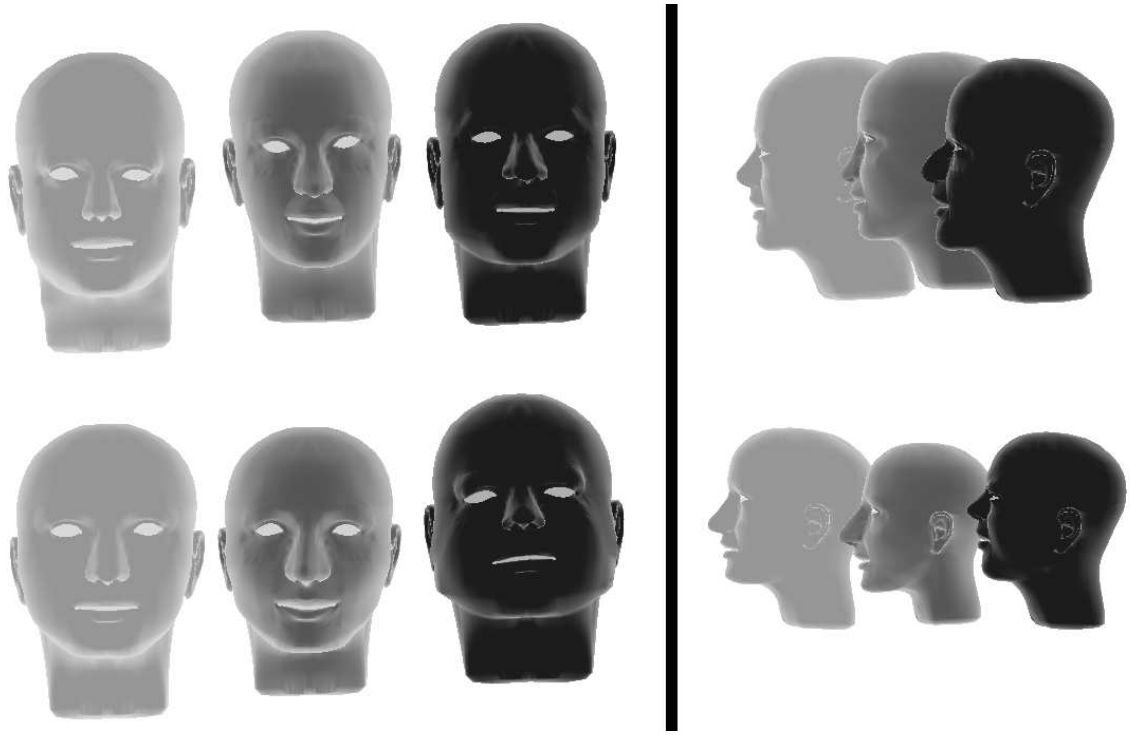

Figure 7. 6 of the 15 faces from the database. The template similarity is most seen in the non-deformed part of the generic mesh (cranial vaults and necks)

3. Statistical Model

3.1. Building the statistical model

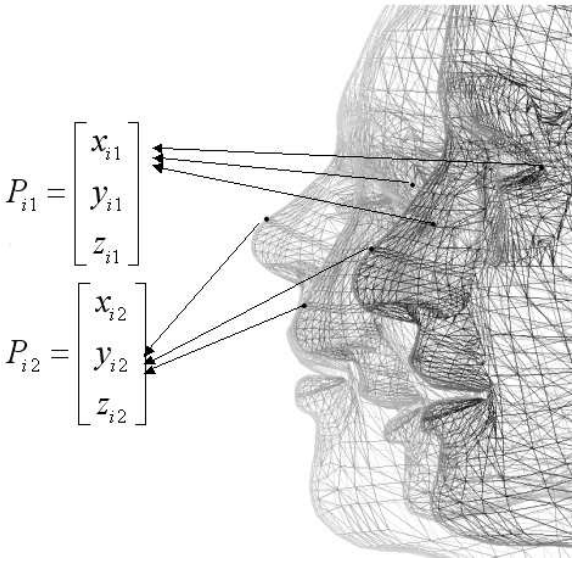

Figure 8. Each vertex of the subject-specific meshes is considered as the same location reflecting thus the inter-individual variations of shape.

Each vertex of the subject-specific mesh is supposed to be a semi-landmark [11] of the 3D surfaces – see Figure 8 for facial fleshpoints – reflecting thus the inter-individual variations of shape. The statistical model is based on this supposition. It is computed on the common part of the original data (see Figure 9). 15 matched skulls and faces are fitted on mean configuration of the skull using Procrustes normalization [16]. 7 degrees of freedom due to initial location and scale are retrieved by this fit (three due to translation along three axes, three due to rotations about three axes, one for scale adjustment). As the fitting is based on mean skull configuration of the skull, the relationships between each face and skull are conserved.

A statistical model of the (partial) skull and the face is then built using Principal Component Analysis (PCA). The result of the PCA is a geometrically averaged facial template, which is computed together with a correlation-ranked set of modes of principal variations based on inter-subjects variations. Principal Component Analysis is an orthogonal basis transformation, where the new basis is found by diagonalising the covariance matrix of a dataset.

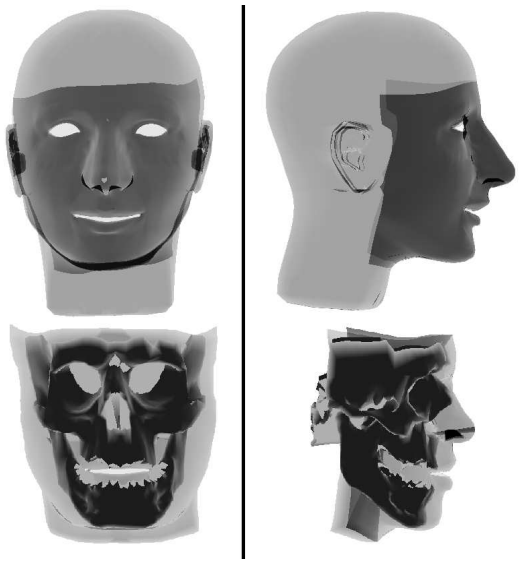

Figure 9. Minimum fitting volumes face vertices (high) and minimum fitting meshes (low).

Let $X_i = (x_{i1}, y_{i1}, z_{i1}, ..., x_{in}, y_{in}, z_{in}) \in R^{3n}$ be the locations of n vertices of the normalized meshes. Using PCA, we can write $T \approx \tilde{T} + \Phi b$, where $\tilde{T}$ is the mean mesh of the skull and face, $\Phi = (\phi_1 | ... | \phi_t)$ is a $(n+m)\times(n+m)$ matrix composed with the eigenvectors of the covariance matrix S of the centered data and b is a vector of t dimension : $b = \Phi^t (T_i - \overline{T})$.

The dimension t of the vector b is the number of eigenvectors with the largest eigenvalues. In classical use of PCA, such as de-noising, t is chosen by $\sum_{i=1}^{t} \lambda_i \geq 0.95 \sum_{i=1}^{m+n} \lambda_i$. The vector b is then a good approximation for the original dataset and any of $n+m$ points can represented or retrieved with the $t_{t<n+m}$ values of the vector b by $T \approx \tilde{T} + \Phi b$

3.2. Results

Every entry in the database is parameterised as a function of the statistical model. Instead of using a vector description of densely sampled points and skull landmarks, the entry is modelled as well as the sum of the geometrically averaged entry and a weighted linear combination of the modes of principal variation by $\tilde{T}+\Phi b$ with a fewer number of parameters. By altering the parameters b, new synthetic but plausible skulls and faces, lying within the statistical boundaries of the mode,l are generated.

In our case, with 15 subjects, a total of 13 variations can be computed, since a leave-one-out approach is used to test the generalization of the modeling procedure. Only

the first eight modes of variations (see Table 2) are significant in terms of represented variance.

Table 2. Percentage of cumulative variance explained.

Mode number	1	2	3	4	5	6	7	8
Cumulative variance	36	51	64	73	79	84	88	91

The accuracy of this model is tested by reconstruction : for a given mesh, variation modes or parameter vector b are computed by minimization of the distance between the true real mesh T and reconstructed mesh from b : $\widetilde{T}+\Phi b$. The mean reconstruction errors (figure 10) for the last three modes are below the millimeter for samples of the learning database. So the reconstruction is quite accurate with sample in the learning database. Reconstruction error for a test sample i.e. a sample which is not in the learning database, is around 3.85 mm for the skull and 3.25 mm for the face for the last four modes. The skull reconstruction is mostly determined by the first variation as the reconstruction error is then around 4.2 mm.

These two results demonstrate that this method seems promising but that the number of samples in the learning database is too small.

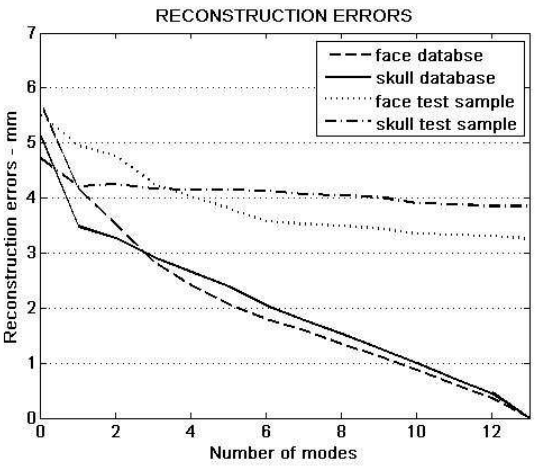

Figure 10. Mean reconstruction errors of the skull and face using an increasing number of mode

Except for the first variation mode, the principal variations of the shape explained by the model are a little more descriptive of the variation of the face shape than those of the skull shape. It can be linked to the greater number of vertices belonging to the face (3780) than to the skull (2900) (Table 3).

Table 3. Percentage of cumulative variance explained for each part of the model (face, skull) for the first 6 modes.

Mode number / Cumulative variance	1	2	3	4	5	6
face	36	50	64	75	82	86
skull	39	48	59	66	72	79

Figure 11 and 12 present the variations of the skull and face shape according to the first modes for parameters varying between +3 and –3 times the standard deviation. The first parameter influences variations of the face and skull width, while the second parameter models the face and skull height. The third parameter influences the shape of the nose as well as the ratio between the upper and the lower parts of the face. Parameters four influences the shape of the nose and parameter five is linked to the shape of the jaw. The first five modes of variations represent 73 percents of the cumulated (Table 2). As the mandible position is different for each subject, each mode of variations models the jaw aperture (Figure 12).

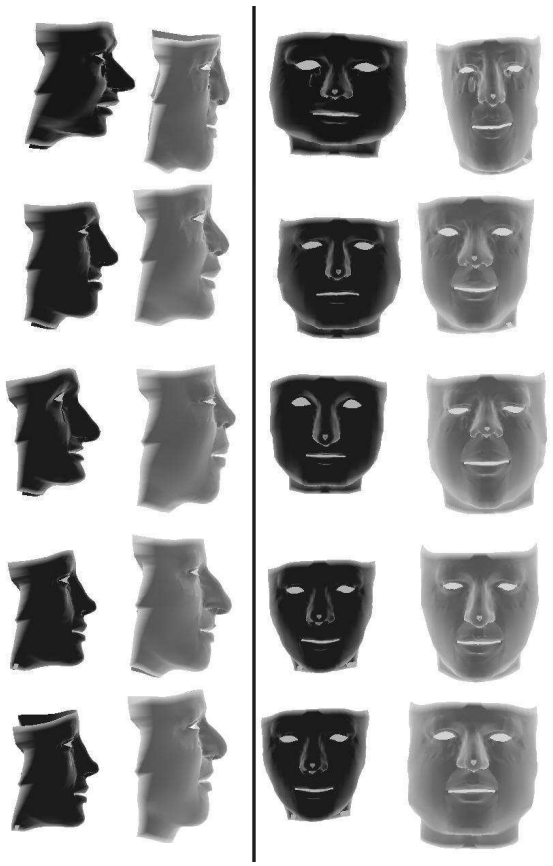

Figure 11. Variations of the face shape according to the first 5 modes for parameters varying between +3 and –3 times the standard deviation.

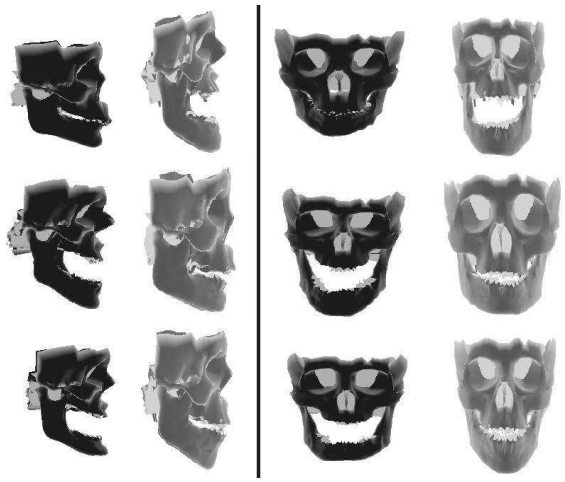

Figure 12. Variations of the skull shape according to the first 3 modes for parameters varying between +3 and –3 times the standard deviation.

4. Statistical Reconstruction

4.1. Missing Data Extension

The linear PCA model defined here can be extended in an elegant way in order to take into account spatial relations between landmarks and to estimate an unknown part of a partially visible or occulted model [17].

Under this hypothesis, if some points (says $t=n$ points) are known, the remaining unknown points are determined using PCA. Without any approximations, we can write:

$$\begin{bmatrix} C_1 \\ \vdots \\ C_n \\ X_1 \\ \vdots \\ X_m \end{bmatrix} = \begin{bmatrix} \overline{C}_1 \\ \vdots \\ \overline{C}_n \\ \overline{X}_1 \\ \vdots \\ \overline{X}_m \end{bmatrix} + \begin{bmatrix} \Phi_{1,1} & \cdots & \Phi_{1,n+m} \\ \vdots & \ddots & \vdots \\ \Phi_{n+m,1} & \cdots & \Phi_{n+m,n+m} \end{bmatrix} \begin{bmatrix} b_1 \\ \vdots \\ b_n \\ b_{n+1} \\ \vdots \\ b_{n+m} \end{bmatrix}$$

This is a linear system with $n+m$ equations and unknowns that can not be resolved. Since PCA can represent the dataset with $t<n+m$ values, suppose $t=n$, the unknown vector $(b_1,\ldots,b_n,X_1,\ldots,X_m)$ in the following system. Notice, that if we choose t<n, the system becomes overdetermined and a least square method can be used to resolve the system :

$$\left\| \begin{bmatrix} C_1 - \overline{C}_1 \\ \vdots \\ C_n - \overline{C}_n \\ -\overline{C}_{n+1} \\ \vdots \\ -\overline{C}_{n+m} \end{bmatrix} - \begin{bmatrix} \Phi_{1,1} & \cdots & \Phi_{1,t} & 0 & \cdots & \cdots & 0 \\ \vdots & \vdots & \vdots & \vdots & \vdots & \vdots & \vdots \\ \Phi_{n,1} & \cdots & \Phi_{n,t} & 0 & \cdots & \cdots & 0 \\ \Phi_{n+1,1} & \cdots & \Phi_{n+1,t} & -1 & 0 & \cdots & 0 \\ \vdots & \vdots & \vdots & 0 & \ddots & \vdots & \vdots \\ \vdots & \vdots & \vdots & \vdots & \vdots & \ddots & 0 \\ \Phi_{n+m,1} & \cdots & \Phi_{n+m,t} & 0 & \cdots & 0 & -1 \end{bmatrix} \begin{bmatrix} b_1 \\ \vdots \\ b_n \\ X_n \\ \vdots \\ X_{n+m} \end{bmatrix} \right\|^2$$

In this framework, a linear approximation of spatial relations between known and unknown points is explicitly determined from the eigenvectors of the covariance matrix.

4.2. Statistical Facial Reconstruction

Using the extension of the linear PCA defined above, the face of a subject can be reconstructed from his skull and from the statistical model defined previously. The known part (Ci) contains the skull vertices while the unknown part (Xi) contains the face vertices.

A leave-one-out approach is used to test the accuracy of the facial reconstruction. The learning database is composed of all subjects minus one, which is the test sample. Every subject becomes the test sample in turn. Figure 13 gives the mean reconstruction error of the test sample which is not part of the learning base. It also gives the reconstruction error for the samples of the learning database.

In all cases, the global reconstruction is correct. The face and skull are reconstructed with an accuracy of 0.5 mm for the samples in the learning database. Test face sample is reconstructed with a mean accuracy of 6 mm. Clearly, these results show that the method is promising but suffers from the size of the learning database. The first parameter offers a better approximation of the reconstructed face with a mean reconstruction error of 5.2 mm. As the skull provides essentially the first mode of variation (see figure 10) and the other modes are mostly related to variations of the face for our test sample, only the result for the first parameter can be considered. For each variation mode after the first one, the prediction can not be considered as it infers variations of the face from variations not taken into account for the skull, the values of the variations modes being not accurate. As these parameters don't correspond to variation modes with null eigenvalues, a large error in their prediction results in a large error in reconstruction.

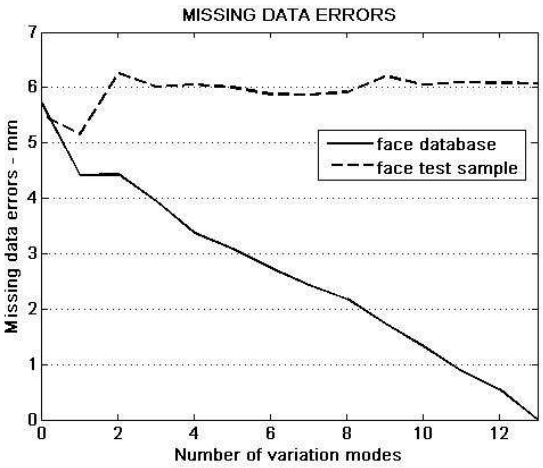

Figure 13. Mean Facial Reconstruction errors using an increasing number of modes.

The repartition of the missing data errors on the face is shown figure 14. Large errors are located on the cheeks, on the neck and on the sides of the nose. It is important to note that the cheeks are not attached to the skull and that the database provides different mandible positions. So, it is very difficult to predict correctly the position of the vertexes of the cheeks. Moreover, the density of vertexes for the cheeks region is quite low, which enables a sliding of those points. The neck is unconnected to the skull, so large errors are inescapable. Last, to predict the shape of the nose knowing the shape of the skull is very difficult [18, 19]. The links between the two organs are complex. These errors located on the sides of the nose are probably due to this situation. The good reconstruction of the tip of the nose can be conversely associated to the template used during the creation of the database.

By using a smaller bounding box that excludes the tip of the nose and the neck, we are able to gain half a millimeter in the accuracy of the prediction (to 4.6 mm). The maximal error is reduced from 3 mm as seen in figure 15.

Two limitations of the current database are its small size, the non homogeneity of the face mesh (the regions of the nose and the lips are much more dense than the rest of the mesh) and the coarseness of the skull mesh. The following parts present two ways of compensating for these limitations. One way is to create a synthesis database using the matching algorithm to simulate virtual shape variations on the meshes. The other way is to use a decimated mesh of the face (with a more homogenous distribution of the vertices) which will indirectly give more weight to the skull vertexes in the statistical model.

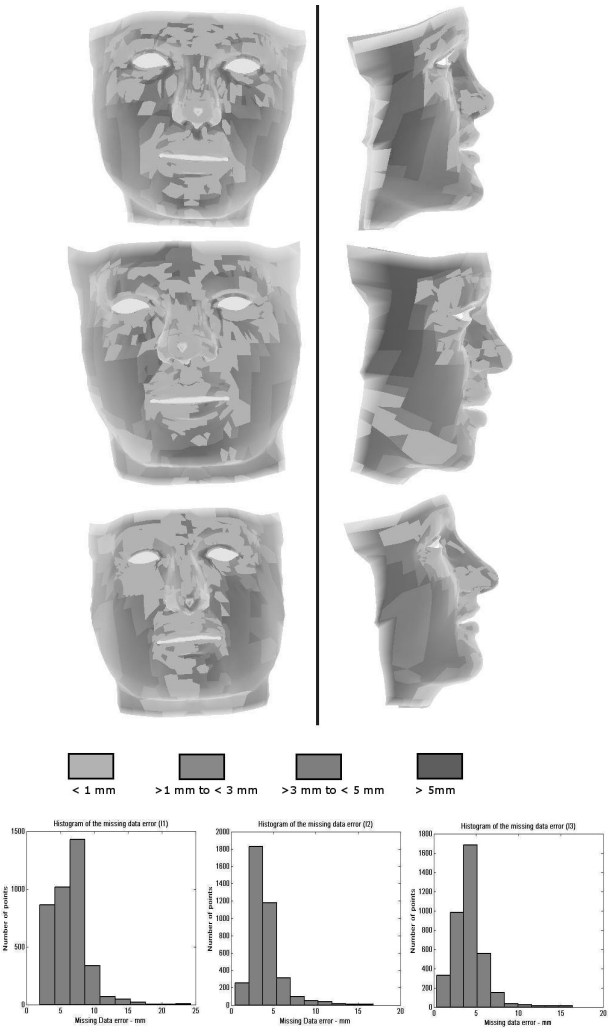

Figure 14 : Distance maps and histograms of the facial reconstruction error for 3 reconstructed faces.

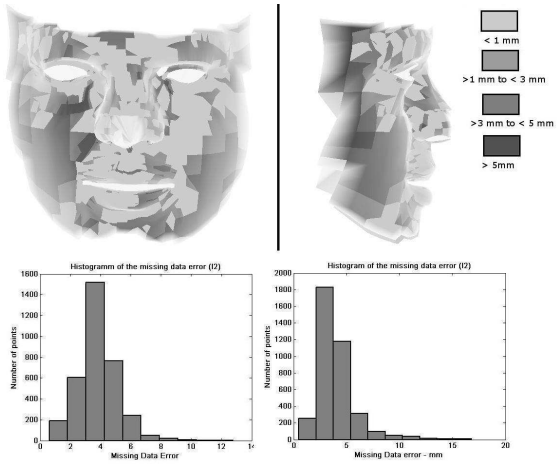

Figure 15**.** Distance maps and histograms of the facial reconstruction error for a reconstructed face using the enclosed model (no neck or tip of the nose) (left) and the original model (right).

4.3. Decimated Facial Reconstruction

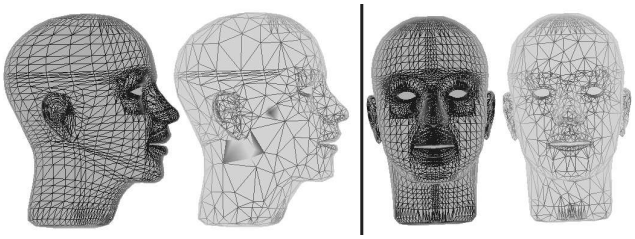

Figure 16. Original and decimated face meshes.

A decimated face mesh (929 vertices) is extracted from the original mesh (3780 vertices). As the decimated mesh is a subpart of the original mesh, every entry of the database can be expressed with only the vertices belonging to the decimated mesh. Each vertex of the decimated mesh represents a larger area of the face. The skull vertices now represents 75% of the vertices of the model.

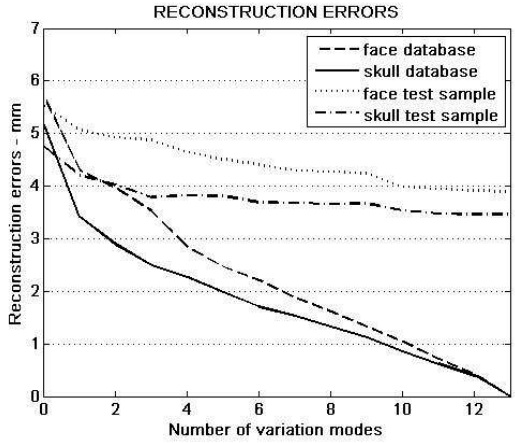

Figure 17. Mean reconstruction errors of the skull and face using an increasing number of mode for the decimated model.

The accuracy of this decimated model is first tested by global reconstruction. The mean reconstruction errors (figure 17) for the last three modes are below the millimeter for samples of the learning database as with the original mesh. The reconstruction is quite accurate with sample in the learning database. Reconstruction error for a test sample is around 3.6 mm for the last four modes. These results are similar to those of the non-decimated mesh. The reconstruction of the skull test sampled is now determined essentially by the first three modes of variations. These modes see the cumulative explained variance be more descriptive of the skull shape variations than the face shape variations (Table 4).

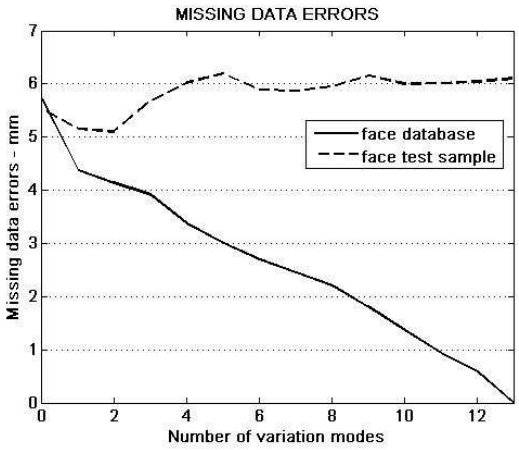

Figure 18. Mean Facial Reconstruction errors using an increasing number of modes for the decimated model

Table 4. Percentage of cumulative variance explained for each part of the model (face, skull) for the first 6 parameters.

Mode number / Cumulative variance	1	2	3	4	5	6
Face + skull	38	55	65	72	78	83
face	31	40	50	63	71	76
skull	41	59	68	72	78	83

Here again, the reconstruction of the face using the missing data extension of the PCA is promising (figure 18). The face is reconstructed with an accuracy of 0.6 mm for the samples in the learning database. Test samples are reconstructed with a mean accuracy of 6.0 mm. As with the original model, the first variation mode offers a better approximation of the reconstructed face with an error of 5.1 mm. As there are more skull vertexes than face vertexes in the decimated model, the first two parameters give now an adequate information for the prediction of the face. The distribution on the face of the facial reconstruction error is similar to the original model (see figure 19).

In conclusion, the "decimated" model gives similar results to the "global" model (the gain is 0.1 mm for the facial reconstruction with 2 valid modes). However these results show that the more accurately the skull will be parameterised by the model (i.e. the greater the number of valid variation parameters), the more accurately the face will be predicted, as the error on these parameters determining the skull will not interfere on the prediction of the face.

One other mean of increasing the number of valid variation modes is to increase the size of the database.

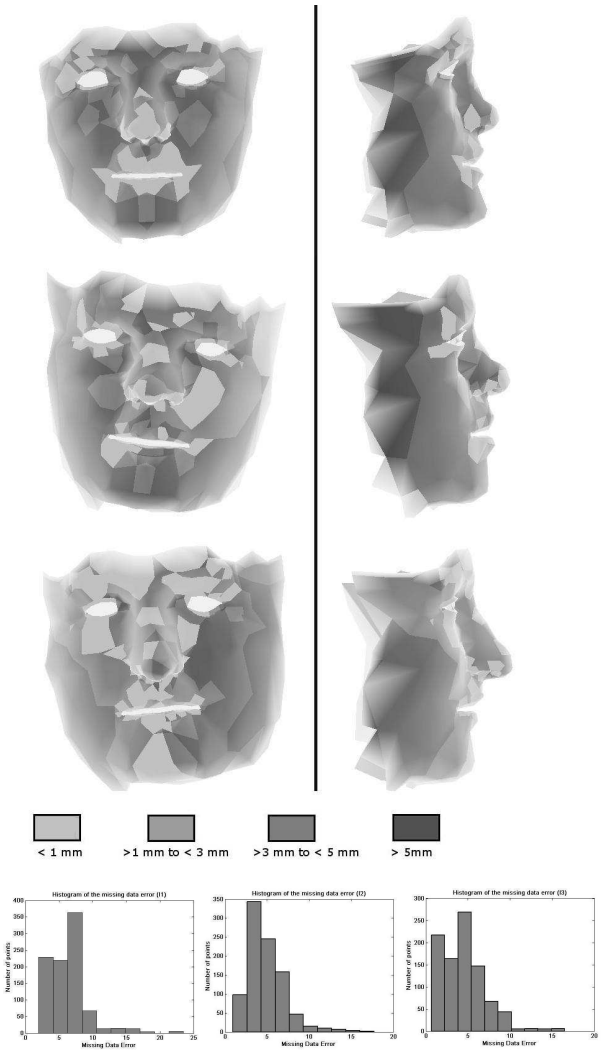

Figure 19**.** Distance maps and histograms of the facial reconstruction error for 3 reconstructed decimated faces.

4.4. Synthetic Facial Reconstruction

A synthetic skull and face database is built using one of the original individual and a set of elastic transformations defined as an octree. Random transformations of the cube enclosing the two meshes were provided, thus transforming the two meshes. The transformations used are defined by the variations of the position of the nodes of the octree. The transformation so defined is relatively smooth as only one level of subdivision is used. Figures 20 respectively illustrate the five parameters that are used to deform the meshes: three scaling parameters, and variations of the center of the X face and of the central axis of the cube (Z direction). Of course, these variations can't simulate the reality of the skulls and faces variability. However, it is a way to artificially verify the missing data formulation and the semi-landmark hypothesis.

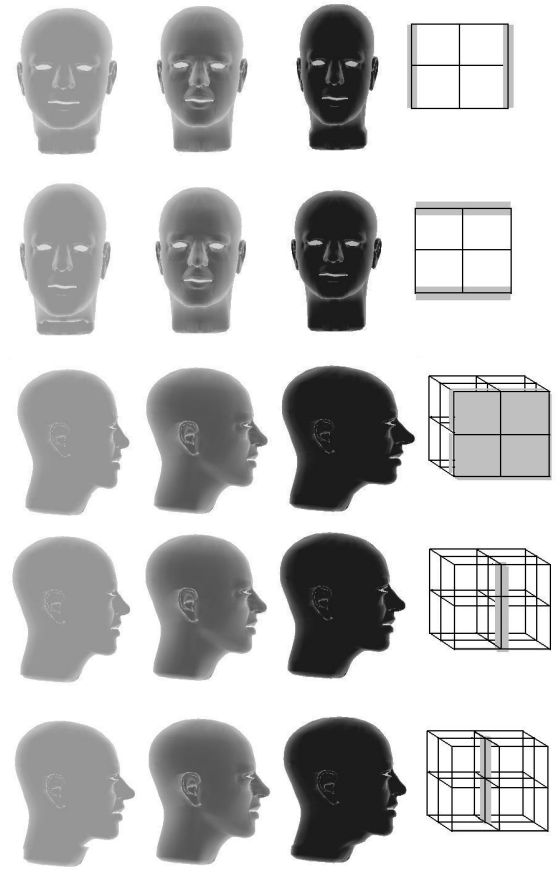

Figure 20. transformation zones and meshes for the 5 deformation parameters.

One hundred set of meshes are generated using these random transformations. To further increase the variability on the face, a Gaussian noise is added to each point. The level of this noise is chosen so that we still remain in the semi-landmark paradigm. Indeed, a large level of noise could change the relative positions of the vertexes of the mesh, thus making the concept of semi-landmark not valid anymore.

A 2mm value was chosen for the level of noise. **Erreur ! Source du renvoi introuvable.** and **Erreur ! Source du renvoi introuvable.** plot the reconstruction results.. Test samples are reconstructed with a mean accuracy of 1 mm. The missing data error is in the same range. It is important to note that the missing data error converges to the reconstruction error for the known part of the test sample (the skull) as well as for the unknown part (the face). If the level of noise is increased, the accuracy of both the reconstruction and the missing data errors augment. Results equivalent to the previous models are encountered for a 5 mm added Gaussian noise. At this level of noise, the semi-landmark paradigm is not valid anymore.

If the subject-specific meshes are used as test samples on the synthesis database, bad reconstructions are obtained for each individual as the variations of the

shapes used are too simple. However, if each subject-specific mesh is deformed using this set of transformations, we guess that it would be possible to obtain a better face and skull model, because of the higher number of degrees of freedom introduced by the synthesis.

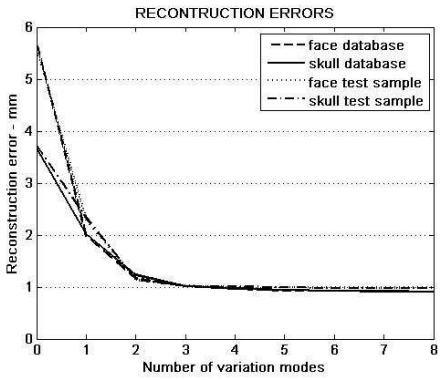

Figure 21. Mean reconstruction errors of the skull and face using an increasing number of mode for the synthesis database model.

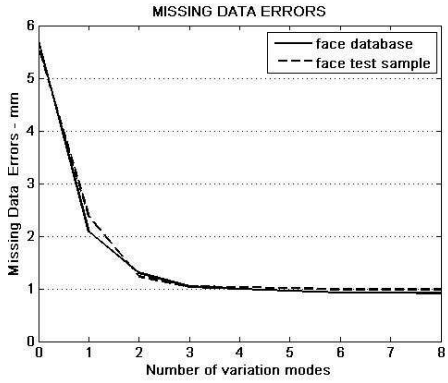

Figure 22. Mean Facial Reconstruction errors using an increasing number of modes for the synthesis database model.

5. Conclusion

In this paper, a face and skull statistical model is proposed for 3D computerised facial reconstruction. To build this statistical model, a 3D-to-3D matching procedure delivers subject-specific meshes of the skull and face with the same number of vertices. A shared normalized space for the faces and skulls is therefore built. The direct statistical relationships between the face and the skull included in the statistical model are used to reconstruct the missing data of the face when the skull is the only available information. For this, a missing data extension of the Principal Component Analysis is used.

Results are visually correct and mean measured errors show that the method is promising as it will be probably more efficient for larger learning database. Two ways of increasing the efficiency of the model are presented. The first one consists in decimating the face mesh in order to adjust its density to the skull mesh density, thus giving a higher weight to the known part of the problem, i.e. skull data. The corresponding results are similar to the ones provided by the original model (at least in term of facial reconstruction), but a slightly more efficient modeling of the skull was observed. The other method to improve the efficiency of the model consists in creating smooth elastic transformation to artificially increase the side of the database. As this database is synthetic, with up to now very simple non-linear transformations, the first results are quite coherent. Further works should provide more complicated elastic transformations applied to a larger database

Acknowledgment

CT scans and MRI data have been collected for several subjects thanks to the maxillofacial department of Toulouse Hospital, with a grant from the BQR/INPG “Vésale”. We acknowledge Praxim-Medivision SA for the use of the initial 3D-to-3D matching software.

References

[1] P. Vanezis, Application of 3-D computer graphics for facial reconstruction and comparison with sculpting techniques.” Forensic Science International, 42 (1989), pp. 69-84.

[2] P. Vanezis, M. Vanezis, G. McCombe, T. Niblet, Facial reconstruction using 3-D computer graphics. Forensic Science International, 108 (2000), pp. 81-95.

[3] R. Evenhouse, M. Rasmussen, L. Sadler, Computer-aided Forensic facial reconstruction. Journal of BioCommunication, 19.2 (1992), pp. 22-28.

[4] A.W. Shahrom, P. Vanezis, R.C. Chapman, A. Gonzales, C. Blenkinsop, M.L. Rossi, Techniques in facial identification : computer-aided facial reconstruction using laser scanner and video superimposition. International Journal of Legal Medicine, 108 (1996), pp. 194-200.

[5] A. J. Tyrell, M.P. Evison, A.T. Chamberlain, M.A. Green, Forensic three-dimensional facial reconstruction : historical review and contemporary developments. Journal of Forensic Science 1997; vol. 42(4): pp. 653-661.

[6] G. Quatrehomme et al, A fully three-dimensional method for facial reconstruction based on

deformable models. Journal of Forensic Science, 42.4 (1997), pp. 649-652.

[7] L.A. Nelson, S.D. Michael, The application of volume deformation to three dimensional facial reconstruction : a comparison with previous techniques. Forensic Science International, 94 (1998), pp. 167-181.

[8] M.W. Jones, Facial reconstruction using volumetric data. Proceedings of the 6th International Vision Modeling and Visualisation Conference, (2001), pp. 21-23, Stuttgart, Germany.

[9] D. Vandermeulen, P. Claes, P. Suetens, S. De Greef, G. Willems, Volumetric deformable face models for cranio-facial reconstruction. Proceedings of the 4th international symposium on image and signal processing and analysis - ISPA, (2005), pp. 353-358, Zagreb, Croatia

[10] P. Claes, D. Vandermeulen, S. De Greef, G. Willems, P. Suetens, Statistically deformable face models for cranio-facial reconstruction. Proceedings of the 4th international symposium on image and signal processing and analysis - ISPA, (2005), pp. 347-352, Zagreb, Croatia

[11] F. L Bookstein. Landmark methods for forms without landmarks: morphometrics of group differences in outline shape. Medical Image Analysis, 1 (1997), pp. 225-243.

[12] W. E. Lorensen, H. E. Cline. Marching cubes: A high resolution 3D surface construction algorithm. Computer Graphics, 21 (1987), pp. 163-169.

[13] R. A. Banvard, The Visible Human Project® Image Data Set from Inception to Completion and Beyond. CODATA 2002 : Frontiers of scientific and technical data, Track I-D-2: Medical and Health Data, (2002), Montreal, Canada

[14] F. Pighin, J. Hecker, D. Lischinski, R. Szeliski and D. H. Salesin, Synthesizing Realistic Facial Expressions from Photographs. Proceedings of Siggraph, (1998), pp 75-84, Orlando, FL, USA.

[15] B. Couteau, Y. Payan, S. Lavallée, The Mesh-Matching algorithm : an automatic 3D mesh generator for finite element structures. Journal of Biomechanics, 33 (2000), pp.1005-1009.

[16] R. Szeliski, S. Lavallée, Matching 3-D anatomical surfaces with non-rigid deformations using octree-splines. International Journal of Computer Vision, 18 (1996), pp. 171-186.

[17] M. Berar, M. Desvignes, G. Bailly, Y. Payan, 3D meshes registration: application to skull model, Proceedings of the International Conference on Image Analysis and Recognition - ICIAR, (2004), vol. 2.:pp 100-107, Porto, Portugal.

[18] M. Moshfeghi. Elastic Matching of Multimodality Images. Graphical models and Processing, 53 (1991), pp. 271-282.

[19] I. L. Dryden, K. V. Mardia; Statistical Shape Analysis. John Wiley and Sons, London, United Kingdom, 1998

[20] B. Romaniuk , M. Desvignes, M. Revenu, M.-J. Deshayes, Shape Variability and Spatial Relationships Modeling in Statistical Pattern Recognition, 25 (2004) Pattern Recognition Letters, pp. 239-247.

[21] C. Basso, T. Vetter, Statistically Motivated 3D Faces Reconstruction. Proceedings of the 2nd International Conference on Reconstruction of Soft Facial Parts, (2005), pp. 71, Remagen, Germany.

[22] C. Rynn and C. Wilkinson, An appraisal of established and recently proposed relationships between the hard and soft dimensions of the nose in profile. Proceedings of the 2nd International Conference on Reconstruction of Soft Facial Parts, (2005), pp. 35, Remagen, Germany.

Received: December, 2005
Revised:
Accepted:

Contact address:
Maxime Berar
Laboratoire des Images et des Signaux
961, rue de la Houille Blanche
BP 46
38402 Saint Martin d'Hères
France
e-mail: berar@lis.inpg.fr

Michel Desvignes
Laboratoire des Images et des Signaux
961, rue de la Houille Blanche
BP 46
38402 Saint Martin d'Hères
France
e-mail: michel.desvignes@lis.inpg.fr

Maxime Berar is a doctoral student at LIS, Grenoble. He received an engineer degree in electronics form the "Ecole Nationale Supérieure d'Electronique et de Radioélectricité de Grenoble (ENSERG)" in 2002. His scientific interests include statistical modeling and Kernel methods.

Michel Desvignes is currently professor in computer science at the ENSERG and researcher at LIS. His scientific interests includes image processing and pattern recognition methods.

Gérard Bailly is CNRS researcher since 1986, senior researcher since 1991 and is head of the Talking Machines team at Institute of Speech Communication (ICP), Grenoble.

Yohan Payan is CNRS researcher at The Computer-Aided Surgery group (GMCAO: Gestes Médico-Chirurgicaux Assistés par Ordinateur) of TIMC laboratory, and coordinates the modeling works that are carried out in TIMC.